Forward-and-reverse multidirectional turning: A novel material removal approach for improving energy efficiency, production efficiency and processing quality

Yuanhui Zhang [a], Wei Cai [a,b,*], Yan He [c], Tao Peng [d], Shun Jia [e], Kee-hung Lai [b], Li Li [a]

a. College of Engineering and Technology, Southwest University, Chongqing, 400715, China

b. Department of Logistics and Maritime Studies, The Hong Kong Polytechnic University, Hung Hum, Kowloon, Hong Kong, China

c. State Key Laboratory of Mechanical Transmission, Chongqing University, Chongqing 400030, China

d. Institute of Industrial Engineering, School of Mechanical Engineering, Zhejiang University, Hangzhou, 310027, China

e. Department of Industrial Engineering, Shandong University of Science and Technology, Qingdao, 266590, China

Abstract

To address the issue of high energy consumption and low utilization rate in conventional turning, a concept of forward-and-reverse multidirectional turning (MDT) and the MDT approach are proposed to reduce energy consumption in idle running, improving processing efficiency and overcoming the tool-chip entanglement. The energy consumption characteristics, processing efficiency, chip morphology and surface quality of the MDT are discussed for better understanding on the motion characteristics and superiorities compared to unidirectional turning (UDT). In three practical applications, MDT processing efficiency was increased by 6.40%, 8.45% and 7.76%, and energy consumption was reduced by 10.85%, 7.25% and 9.51%, respectively. In addition, the MDT has better chip removal control ability, which contributes to machining stability. The surface quality of the workpieces processed by the MDT was generally better than that by UDT. Furthermore, this study has theoretical and guiding significance for the application of multidirectional turning in practical production.

Key words: Turning; Energy efficiency; production efficiency; Processing quality; Material removal; Forward-and-reverse multidirectional turning (MDT)

1 Introduction

Climate change caused by excessive carbon dioxide emissions is a global issue facing mankind [1]. In the context of "carbon neutrality" and "carbon peak" [2,3], the manufacturing industry needs to consider the problem of energy conservation and quality balance more meticulously and practically. Machine tools,

highly widespread in machining systems, are the main body of electrical energy consumers with low energy efficiency [4]. At the same time, cutting is the key technology to obtain precision machining and high-quality surfaces of workpiece [5]. The non-cutting operations in a modern turning machine tool usually dominate energy requirements and the energy used in the actual machining only accounts for approximately 15% of the total energy [6]. Compared with developing alternative clean energy sources, improving energy efficiency in current situation is a direct and effective measure due to significant economic barriers [7].

The conventional turning with unidirectional turning has been widely studied. For turning parameter optimization, an approach of optimizing the cutting parameters in the machining process was proposed to balance the carbon emissions, cutting time and cutting cost during the machining of parts, which provides a new way of comprehensive optimization of cutting parameters and tools to reduce carbon emissions [8]. For the non-cutting state, the energy-saving strategies of shortening the air cutting time and infrequently changing the spindle speed were provided [9]. The influence of cutting parameters on the cutting performance of 7075-T651 aluminum alloy under different machining methods was studied [10]. The cutting process of nickel superalloy was studied and the influence of feed and cutting parameters on tool durability and wear was determined [11]. The changes of cutting temperature, cutting force and cutting surface roughness with cutting speed during precision turning of VT1-0 titanium alloy with PCD tool were studied, and the optimal cutting conditions were determined [12]. Taguchi method was used to analyze the influence feed rate and depth of cut on the surface roughness and cutting force of the stainless-steel turning process [13]. The response surface method combined with the finite element method is used to optimize the hard turning process parameters to minimize the machining force and white layers thickness [14].

For energy consumption modeling, which has been recognized as an effective analytical method and management tool for enhancing energy efficiency [15]. A new model was proposed to characterize power loss due to cutting load, and the power losses of mechanical drives and spindle motors were analyzed and modeled separately [16]. A generic energy model for turning and milling machines and related machining was developed to predict the energy consumption of complex parts with turning and milling characteristics. The prediction model was applicable to high precision high-end turning and milling machines and was validated by two examples [17]. The power prediction methods in the turning process were studied, and three methods based on the specific energy method, the cutting force-based method

and the exponential function-based method were considered comprehensively [18]. A predictive modeling method based on machine tool operation history data is proposed. The method allows for a variety of power consumption prediction models for different machining structures [19]. The empirical model for energy consumption prediction and the back propagation neural network prediction model were established respectively, and the power signal measurement system was built on a computer numerical control lathe and verified in the machining process of 45 steel [20]. A prediction model for the specific energy consumption and surface roughness of the machine tool considering the evolution of tool wear was developed, and the proposed model was validated by wet turning tests on AISI 1045 steel [21]. An energy consumption model for the drilling process was proposed. The proposed energy consumption model includes idle power, cutting power and auxiliary power, and the cutting power in the drilling process was obtained using the cutting force [22]. Based on the principle of spindle motor control, the energy consumption model of CNC lathe spindle acceleration was established, and potential methods to reduce this part of energy consumption were discussed [23]. Various experimental or empirical energy consumption models for spindle acceleration, spindle rotation, feed and material removal were summarized, as well as energy consumption models for the machine tool during material removal [24]. An empirical mode was developed to predict the cutting energy consumption of the variable-power consumption machining process i.e., end facing [25]. A new energy mapping method to evaluate the cutting energy consumption for specific cutting parameters was proposed for energy consumption analysis [26].

For chip morphology, the chip shape characteristics obtained from cutting tests under different cutting conditions were analyzed and compared, and the influence of cutting parameters on the force, temperature and stress on the shear surface was revealed [27]. Based on chip breaking conditions and chip breaking dot position conditions, the theoretical location area of the laser cladding chip breaking point on the rake face of the tool is determined [28]. The finite element method was used to simulate sinusoidal spindle speed variation and constant speed machining, and the chip formation mechanism during Ti6AI4V processing is studied [29]. Through orthogonal cutting experiments, the chip formation process of Ti 6AI 4V alloy at high cutting speed and large uncut thickness was studied [30]. Orthogonal experiments were carried out using high-speed camera recording and simultaneous measurement of cutting force to analyze the chip formation in the vibration process of the machine tool [31]. Under high loadings, the chip formation mechanism, chip morphology and microstructure in the cutting process

were analyzed [32].

For processing efficiency, taking BS EN24T alloy (AISI 4340) as an example, the energy efficiency analysis and optimization were carried out, a multi-objective optimization model was established, and a new and improved multi-group fruit fly optimization algorithm (IMFOA) was proposed to identify the optimal solution [33]. A machining energy consumption (MEC) model considering non-cutting energy consumption (NCEC) and spindle speed variation (SRCE) was developed, and the optimal spindle speed (SRS) and feed rate were obtained by simulated annealing (SA) method [34]. Considering the flexibility of tools and the diversity of cutting parameters, an integrated method for optimizing tools and cutting parameters was proposed achieving a balance between minimal energy consumption and minimal production time [35]. The influence of cutting parameters combination under certain material removal rate was studied, for NC machine tool industry to select the optimal cutting parameters to achieve the minimum energy consumption [36]. The non-cutting energy consumption of the machine tool relationship between processing a specific feature and its front and back features was studied to find the optimal or close to optimal features of a specific part (PFS) [37]. It was proposed to improve the efficiency of cutting edge by improving the tribological properties of multi-component coatings deposited on the tool [38].

The analysis of past studies shows that the existing research mainly focused on the optimization of cutting parameters and the energy conservation strategies for conventional turning. Therefore, the following research gaps still exist:

- Most existing studies are based on unidirectional turning (UDT), and the research on multidirectional turning approach is still in its infancy. The machine idle energy consumption has not been effectively addressed.

- Turning operations cover multiple performance and currently lack an approach that can comprehensively address energy consumption, processing efficiency, chip control and surface quality. For example, when pursuing high surface quality, machine tools often come with the sacrifice of more energy consumption.

With the development of new cutting tools, the forward-and-reverse multidirectional turning (MDT) approach is proposed to fill the abovementioned gap. This approach takes workpiece surface quality and chip control into consideration when pursuing high-efficiency and energy-saving machining. The study provides the following practical and academic contributions:

From a theoretical perspective, based on the energy consumption characteristics analysis of turning process, the energy consumption model of MDT and UDT was established. The production time models of MDT were established based on the comparative analysis of tool paths of workpiece with multiple feature surfaces, thus revealing the efficient and energy saving mechanism of MDT. The machining surface quality and chip control ability of MDT are described from the theoretical study of residual area and chip thickness. The new concept of MDT in the mechanical manufacturing industry was first propounded.

From a practical perspective, this study provides a turning approach which mainly overcomes the idle energy consumption of the cutting tool, and also considers the quality of the workpiece and chip control. The proposed approach provides practical technical support for the realization of multidirectional turning and automatic turning, which effectively solves the idle energy consumption and promotes the effective utilization rate of energy. Furthermore, this approach will enable enterprises to attain more product value with lower production cost, meet the demand of energy conservation and emission reduction, which is an effective way to improve the core competitiveness of enterprises.

2 Forward-and-reverse multidirectional turning (MDT)

2.1 Definition of MDT

In view of the obstacles of processing efficiency, energy consumption and chip breakage in the conventional turning, this study presents the MDT in machining as an ingenious approach for sustainability production. The turning process of MDT is shown in Fig. 1, taking the excircle as an example. The figure shows the position of the same cutting tool at different times. The a_{p1} is the depth of cut during forward turning, and e_1 represents the effective cutting edge. The a_{p2} is the depth of cut during reverse turning, and e_2 represents the effective cutting edge. The effective cutting edge of MDT reverse turning is different from that of forward turning, and the effective cutting edge of reverse cutting is enlarged when a_{p1} equals a_{p2}. It is crucial for cutting heat dissipation and prolonging tool life. The forward turning mechanism of MDT is shown in Fig. 1(a), which is similar to that of UDT except the change of tool angle. The difference is that when the forward turning is completed, the MDT tool feeds a_{p2} to the X axis, and then the reverse turning is performed (Fig. 1(b)). This step omits the tool retraction time of the X-axis

and Z-axis, thus avoiding the energy consumption during the idle running. The MDT is also suitable for machining the end face and bevel surface, and the processing order of reverse turning and forward turning is variable.
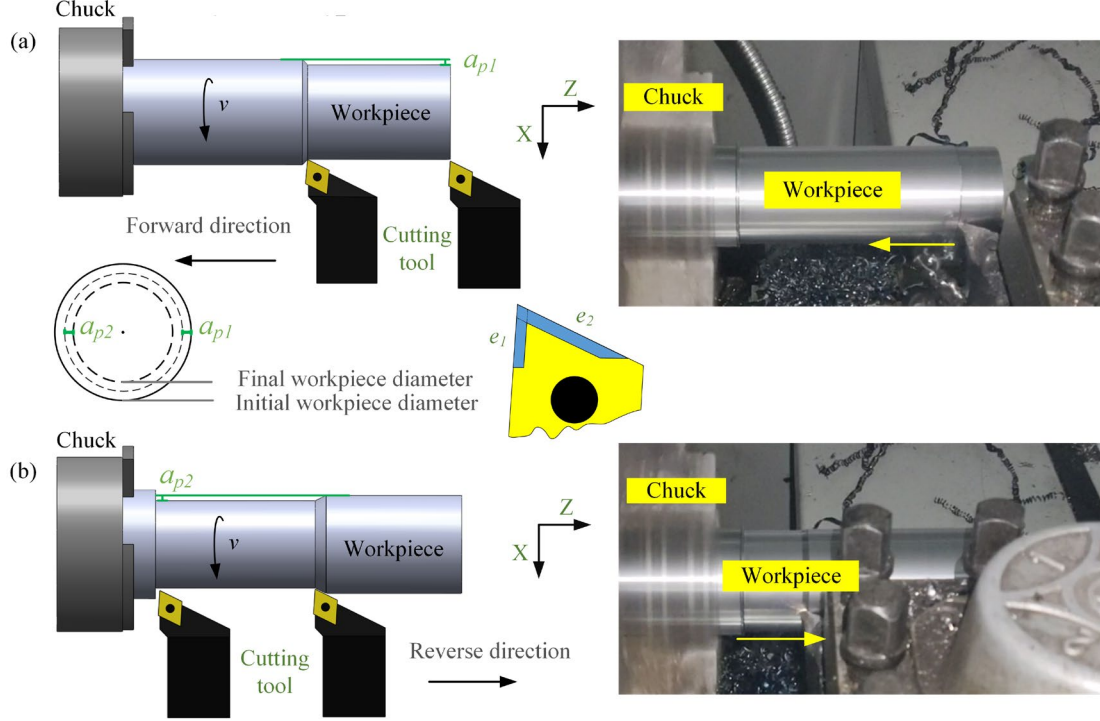

Fig. 1 The machining mechanism of MDT. (a) The machining process of forward turning; (b) The machining process of reverse turning.

2.2 Energy consumption characteristics

During the turning process, the energy consumption of the machine tool mainly includes the energy consumption of standby, start-up, machining, and air cutting [17]. In this study, the machine energy consumption is divided into idling energy consumption and cutting material energy consumption. The comparison of the energy consumption characteristics of MDT and UDT is illustrated in Fig. 2. The total energy consumption of the turning process is expressed by the following equation:

$$E_T = E_{CM} + E_{ID} \tag{1}$$

Where E_T is the total energy consumption, E_{CM} is the cutting material energy consumption, E_{ID} is the idling energy consumption in the process without cutting material. The cutting material energy consumption consists of the following components.

$$E_{CM} = \sum_{i=1}^{N} E_{CMi} \tag{2}$$

Where E_{CMi} is the cutting material energy consumption when machining the i-th feature of the

workpiece, *N* is the feature contained in the machined workpiece. The idling energy consumption consists of the following components.

$$E_{ID} = \sum_{j=1}^{M} E_{IDj} \tag{3}$$

Where E_{IDj} is the idling energy consumption of the j-th idle stage, *M* is the number of idle stages of the tool during one complete processing.

The turning path and energy consumption curve of UDT is shown in Fig. 2(a) and 2(c). The standby energy consumption, start-up energy consumption is the same before cutting starts. The workpiece contains three different features: the excircle, the bevel and the step. In UDT turning, after each feature is processed, the tool is retracted (including segment CD, segment GH, segment JK), which consumes more energy ($E_{ID2}, E_{ID3} \ and \ E_{ID4}$) and time. The turning path and energy consumption curve of MDT is shown in Fig. 2(b) and 2(d). In MDT turning, when the forward turning is done, the MDT will perform a short retraction adjustment (including the CE section, FH section, and JK section), and then the next feature of processing starts. From the starting point of the cut, the MDT completes the machining with only one tool travel.
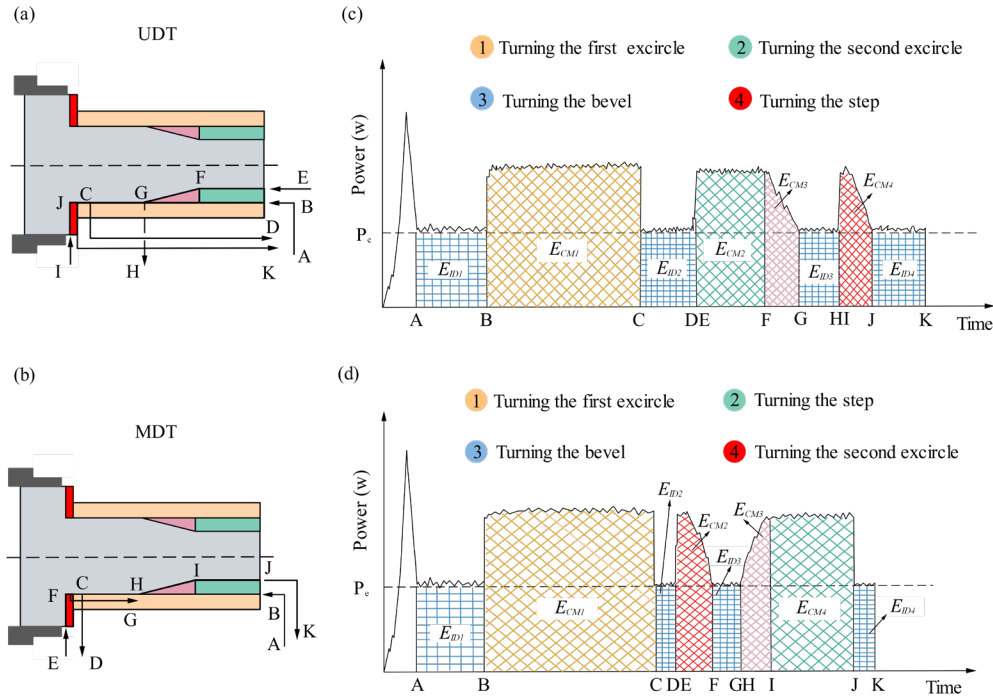

Fig. 2 The energy consumption and turning path. (a) Turning path of UDT; (b) Turning path of MDT; (c) Energy consumption characteristics of UDT; (d) Energy consumption characteristics of MDT.

Through the comparison of turning paths, due to the continuity of the MDT turning path, the idling energy consumption of the tool during the machining process is reduced, the processing efficiency is improved, and the energy consumption of the machine tool is reduced. To facilitate the comparison of

energy consumption between MDT and UDT, an energy efficiency factor Q_e is defined:

$$Q_e = \frac{E_T^{UDT} - E_T^{MDT}}{E_T^{UDT}} \tag{4}$$

Where E_T^{UDT} is the total energy consumption of UDT, E_T^{MDT} is the total energy consumption of MDT.

2.3Processing efficiency

The processing time model are established in this section mainly focuses on processing the excircle for analysis. The processing time flow between UDT and MDT is shown in Fig. 3. After the forward turning of UDT is completed, the tool should be retooled to X axis and then to Z axis to start the next cutting or stop the machining. For MDT, when the number of cuts is even, the machine can be completed without Z-axis retraction, when the number of cuts is odd, it needs to go through Z-axis retraction once. The processing time of MDT and UDT can be expressed by Eq (5).
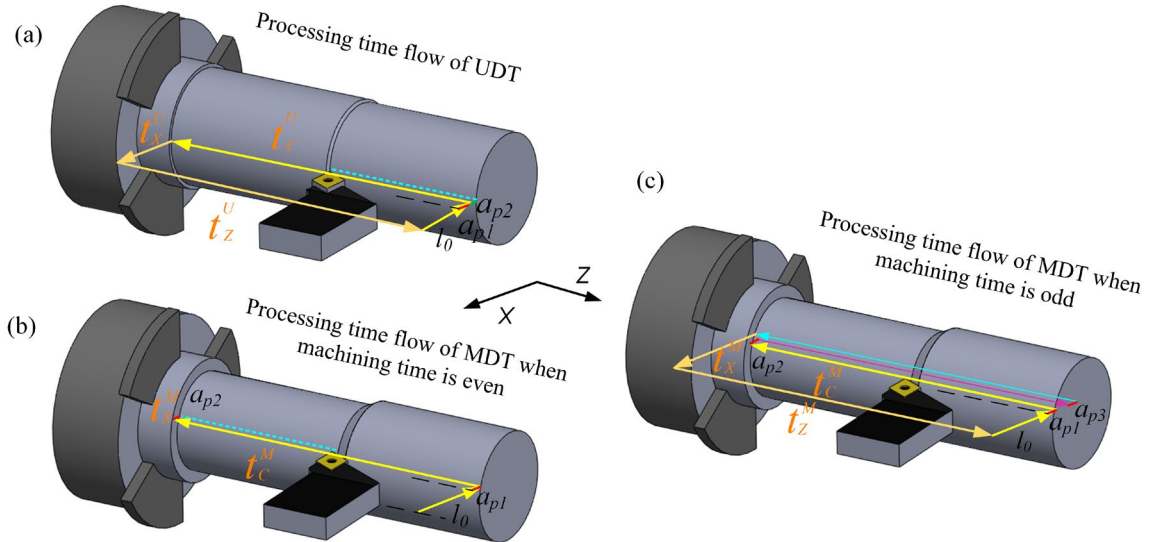

Fig. 3 The comparation of processing time flow between UDT and MDT. (a) The processing time flow of UDT; (b) The processing time flow of MDT when the number of machining is even; (c) The processing time flow of MDT when the number of machining is odd.

$$t = t_C + t_X + t_Z \tag{5}$$

Where t_C is the processing time of material removal, t_X is the retracting and feeding time of the tool on X-axis, and t_Z is the retracting time on Z-axis. For UDT (Fig. 3(a)):

$$\begin{cases} t_C^U = \sum_{i=1}^n \frac{l_i}{60 f_i} \\ t_X^U = \frac{\sum_{i=1}^n (n-i+1) a_{pi} + l_0}{60 f_X} \times 2 \\ t_Z^U = \sum_{i=1}^n \frac{l_i}{60 f_z} \end{cases} \tag{6}$$

For MDT (Fig. 3(b) and 3(c)):

$$
\begin{cases}
t_C^M = t_C^U = \sum_{i=1}^{n} \frac{l_i}{60 f_i} \\
t_X^M = \frac{l_0 + \sum_{i=1}^{n} a_{pi}}{60 f_X} \times 2 \\
t_Z^M = \begin{cases} \frac{l_i}{60 f_Z}, i \in (1,3,5 \dots) \\ 0, i \in (0,2,4 \dots) \end{cases}
\end{cases}
\tag{7}
$$

Where n is the total number of cuts, i is the i-th machining, l_i is the i-th machining length, f_i is the feeding speed of the i-th machining, f_Z is the retraction speed of the Z-axis, f_X is the feeding and retraction speed of the X-axis, a_{pi} is the depth of cut in the i-th machining, and l_0 is the fixed retraction distance of the turning tool. Therefore, the processing time t^U of UDT is:

$$
t^U = t_C^U + t_X^U + t_Z^U = \sum_{i=1}^{n} \left(\frac{l_i}{60 f_i} + \frac{l_i}{60 f_Z} \right) + \frac{\sum_{i=1}^{n} (n-i+1) a_{pi} + l_0}{30 f_X}
\tag{8}
$$

The processing time t^M of MDT is:

$$
t^M = t_C^M + t_X^M + t_Z^M = \begin{cases} \sum_{i=1}^{n} \frac{l_i}{60 f_i} + \frac{l_0 + \sum_{i=1}^{n} a_{pi}}{30 f_X} + \frac{l_i}{60 f_Z}, \ i \in (1,3,5 \dots) \\ \sum_{i=1}^{n} \frac{l_i}{60 f_i} + \frac{l_0 + \sum_{i=1}^{n} a_{pi}}{30 f_X}, \ i \in (0,2,4 \dots) \end{cases}
\tag{9}
$$

The processing efficiency factor Q_p is:

$$
Q_p = \frac{t^U - t^M}{t^U} = \frac{\sum_{i=1}^{n} \frac{l_i}{60 f_Z} + \frac{\sum_{i=1}^{n}(n-i+1) a_{pi} + l_0}{30 f_X} - \frac{l_0 + \sum_{i=1}^{n} a_{pi}}{30 f_X} - \frac{l_i}{60 f_Z}}{\sum_{i=1}^{n} \left(\frac{l_i}{60 f_i} + \frac{l_i}{60 f_Z} \right) + \frac{1}{30 f_X} \cdot \sum_{i=1}^{n}(n-i+1) a_{pi} + l_0}, \ i \in (1,3,5 \dots)
$$

$$
= \frac{\sum_{i=1}^{n} \frac{l_i}{60 f_Z} + \frac{\sum_{i=1}^{n}(n-i+1) a_{pi} + l_0}{30 f_X} - \frac{l_0 + \sum_{i=1}^{n} a_{pi}}{30 f_X}}{\sum_{i=1}^{n} \left(\frac{l_i}{60 f_i} + \frac{l_i}{60 f_Z} \right) + \frac{1}{30 f_X} \cdot \sum_{i=1}^{n}(n-i+1) a_{pi} + l_0}, \ i \in (0,2,4 \dots)
\tag{10}
$$

The higher Q_p indicates that MDT can process more workpieces in the same cycle than UDT. The processing energy consumption in this study is subject to actual measurement.

2.4 Chip morphology and surface quality

Chip morphology and surface quality are essential factors to be considered in actual machining, which has a considerable impact on process stability. As shown in Fig. 4(a) and (b), under the same depth of cut and feed, the chip thickness h_c decreases and the chip width w increases during reverse turning. The variation in chip thickness and width will affect chip formation and breakage. As shown in Fig. 4(b) and (c), the tool cutting edge angle of reverse turning decreases results in the height of residual area of forward turning is difference that of reverse turning. The difference in residual area will affect surface quality. To reveal the effect of forward turning and reverse turning on chip morphology and surface
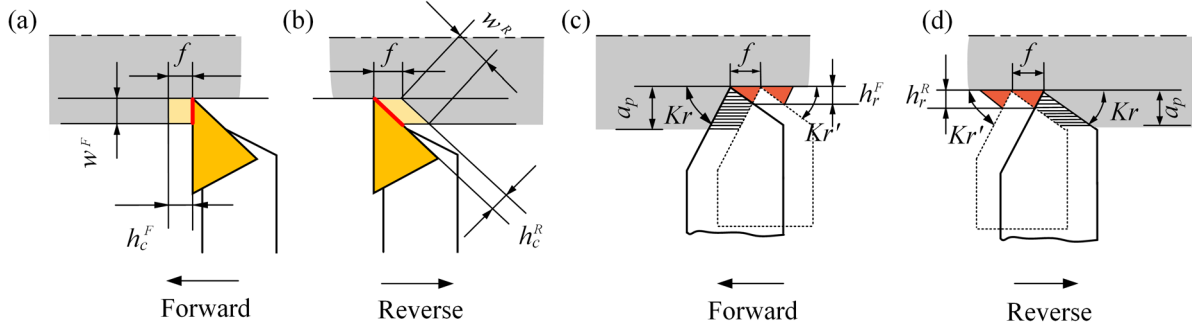
quality, which is a guide for practical operation.

Fig. 4 The analysis of chip morphology and residual area of MDT. (a) Chip morphology of forward turning; (b) Chip morphology of reverse turning; (c) Residual area of forward turning; (d) Residual area of reverse turning.

3 Materials and methods

3.1Scope and objective

Developing new energy-saving processes, optimizing process parameters and process planning is an effective way to optimize energy consumption [39]. This study aims to establish the new processing model in actual machining and reveal its superiority compared to unidirectional turning and to provide theoretical basis and experimental verification for MDT in actual production. The functional unit considered is one workpiece with a rotary surface, which is referred to a typical mechanical manufacturing product. In terms of the mechanical manufacturing industry, the turning cycle of one workpiece is a cradle to grave exercise, namely a process from raw material to finished workpiece. However, in some cases cradle to gate, gate to cradle approaches are possible. For the workpiece, the approach can only be gate to gate as there can be many different applications later. MDT is built based on conventional turning, so it is suitable for whole gate to gate process within the system boundary. In addition, turning processing is a relatively time-consuming processing method in mechanical processing. From rough to finished product, the processing of some complex parts can take up to several hours. The production of large quantities of products requires a long cycle. Therefore, it is strategic to improve the production efficiency and reduce energy consumption of conventional turning based on MDT.

3.2 Devices and methods

Two different experiments were conducted in this study. The first experiment aimed at comparing

the processing efficiency, energy consumption and surface quality of UDT and MDT. The second experiment focused on chip morphology and the surface quality of forward turning and reverse turning of MDT.

The C2-6150HK/1 CNC lathe was used in two sets of experiments, and the maximum machining diameter of the machine tool is 250mm, the rated power of the spindle motor is 7.5KW, and the speed range is 20~1800r/min. ME435 handheld three-phase power energy analyzer was used to measure the power of the machine tool. The data recording frequency set by the measuring instrument is once per second, and the resolution of voltage, current and power is 0.1. The raw material used in the workpiece 1 and 2 and experiments 2 was round bar 45 steel with a diameter of 50 mm and a length of 200 mm. The raw material used in the workpiece 3 was round bar 45 steel with a diameter of 30 mm and a length of 200 mm. No cutting fluid was used in this processing, and dry cutting was performed. The surface roughness of the workpiece is measured by the JB-6C contour roughness meter. The stylus length used is 0.8mm and the sampling length is 20mm. The experiment environment and process are shown in Fig. 5.
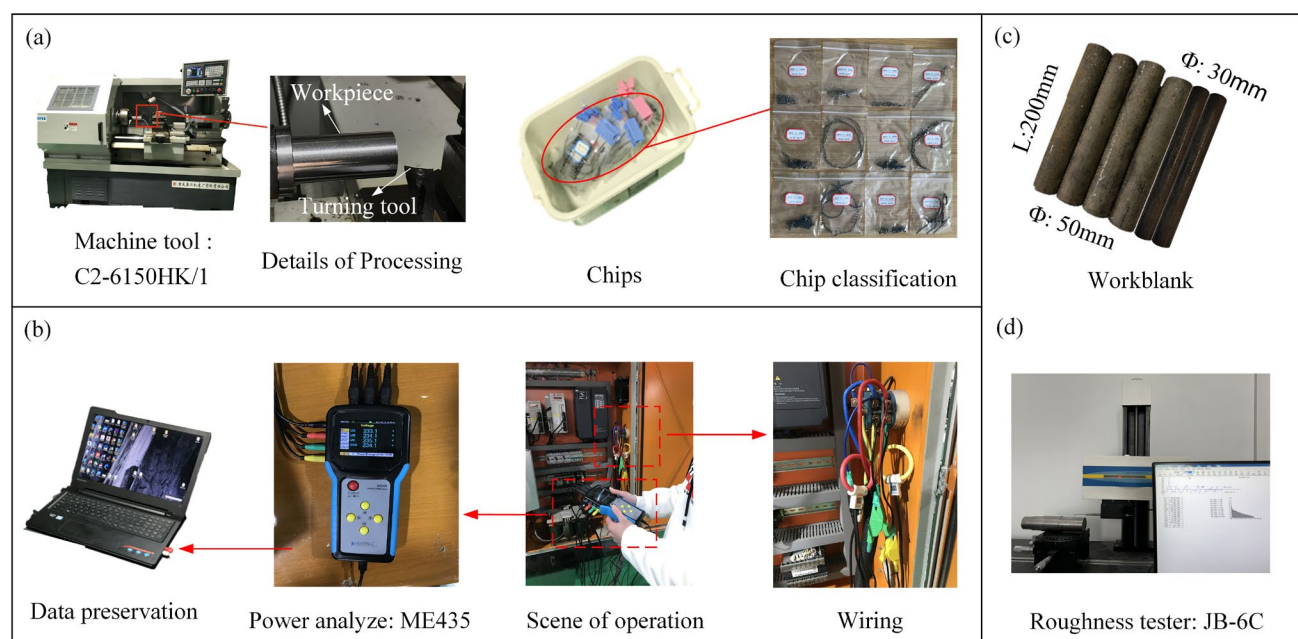

Fig. 5 The experiment site. (a) Machine tool and chip collection; (b) Data collection and wiring; (c) Workblank; (d) Roughness tester.

The MDT tool used in the first set of experiments is CP-B1108-M5 4325, which is a roughing tool. The MDT tool used in the second set of experiments is CP-A1108-L5 4325, which is a finishing tool. The UDT semi-finishing turning tool WNMG080404-MA KT930 was used in two groups of experiments. The main parameters of the tool are shown in Table 1.

Tab.1 The parameters of cutting tool

Group	Approach	Turning type	Tool parameters						Material
			Rake angle γ	Relief angle α	Tool cutting edge angle κ_r	End cutting edge angle $\kappa_{r'}$	Tool cutting edge inclination λ_s	Tip radius	
No.1	MDT	Rough	0°	6°	95°	25°	9°	0.8 mm	
	UDT	semi-finishing	6°	0°	95°	5°	-6°	0.4 mm	Cemented carbide
No.2	MDT	finishing	0°	6°	115°	30°	8°	0.8 mm	
	UDT	semi-finishing	6°	0°	95°	5°	-6°	0.4 mm	

3.2.1 The processing methods and parameters of the first group

In the first set of experiments, MDT and UDT were used to process three shaft parts respectively, while the turning path of the machining process is different. Taking workpiece 1 as an example, the machining process was divided into two sides for processing. When machining the first one workpiece, first processing workpiece of the A-B-C-D surface, and then stop for face-changing, then processing C-D-E-F surface. The energy consumption of the outage process was artificially affected, so it was not included in the energy consumption comparison. On the basis of obtaining machine tool data, it is also necessary to effectively analyze the energy consumption of the machining process according to the properties of the workpiece material and its detailed process parameters. The cutting parameters and turning paths of MDT and UDT when machining the workpiece 1 are shown in the Fig. 6.
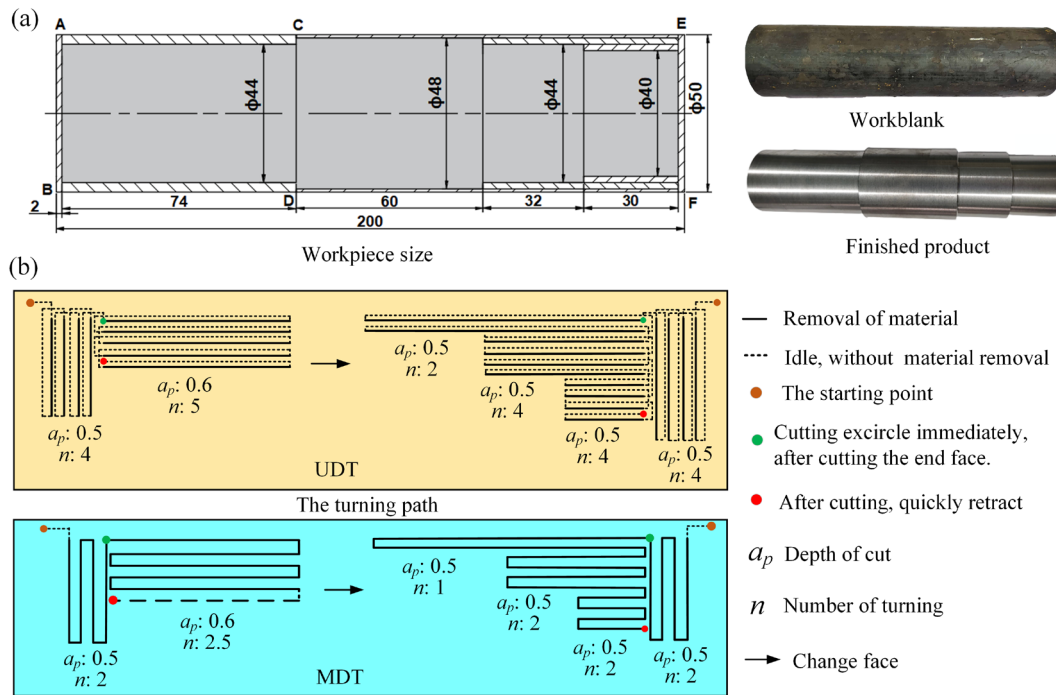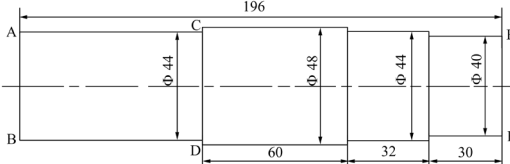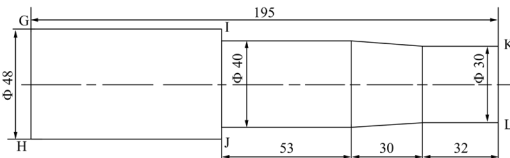

Fig. 6 The comparison of processing technology and path when machining workpiece 1. (a) Processing size of workpiece 1; (b) Comparison of UDT and MDT turning path.

The cutting parameters and turning path selection in the machining process were set according to

the actual production guidelines. The cutting parameters are shown in Table 2, which are consistent with the actual cutting parameters of mechanical production. The spindle speed of the machine was kept at 800r/min, and feeding speed was 0.075mm/r. UDT was one-way turning, and the machining process was divided into two steps. Taking workpiece 1 as an example, when processing the end face of the A-B-C-D surface, the depth of cut is 0.5mm, and it takes four passes to complete the processing. After cutting the end face, the tool returns to the proximal end of the excircle surface and begins to process the excircle with a diameter of 44mm on the A-B-C-D surface, which requires five passes. Then stop the machine to clamp the A-B-C-D face to process the C-D-E-F face. First processing the end face of a 50mm diameter with the same processing steps of the end face of the A-B-C-D face, and then processing the excircle with a diameter of 48mm. Next, an excircle with a diameter of 44mm was machined, and the depth of cut was 0.5mm, four passes were required. Finally, an excircle with a diameter of 40mm was processed, which also requires 4 passes. After the processing was completed, the tool was quickly retracted, and the machine stopped.

Tab.2 The cutting parameters of UDT and MDT

Dimensional drawing of workpiece	Surface	Features	Spindle speed (r/min)	Feeding speed (mm/rev)	Depth of cut (mm)	Cutting number (times)	
						UDT	MDT
Workpiece 1	A-B-C-D surface	End face: Φ50mm			0.5	4	2
		Excircle: Φ44 mm			0.6	5	3
	C-D-E-F surface	End face: Φ50mm	800	0.075	0.5	4	2
		Excircle: Φ48mm			0.5	2	1
		Excircle: Φ44mm			0.5	4	2
		Excircle: Φ40mm			0.5	4	2
Workpiece 2	G-H-I-J surface	End face: Φ50mm			0.5	4	2
		Excircle: Φ48 mm			0.5	2	1
	I-J-K-L surface	End face: Φ50mm	800	0.075	0.5	4	2
		Excircle: Φ40 mm			0.6	9	5
		Bevel and Excircle: Φ30 mm			0.6	9	5
Workpiece 3	M-N-O-P surface	End face: Φ30mm	800	0.075	1	2	1
		Excircle: Φ28 mm			0.5	2	1

Workpiece 1 dimensions: 196; Φ44, Φ48, Φ44, Φ40; 60, 32, 30. Points A, C, E, B, D, F.

Workpiece 2 dimensions: 195; Φ48, Φ40, Φ30; 53, 30, 32. Points G, I, K, H, J, L.

	Excircle: Φ26 mm	0.5	2	1
	Excircle: Φ24 mm	0.5	2	1
O-P-Q-L surface	End face: Φ30mm	1	2	1
	Excircle: Φ26 mm	0.5	4	2
	Excircle: Φ24 mm	0.5	2	1

The machining process of MDT also needs carrying out in two steps. The end surface with a diameter of 50mm was processed first. When the first pass of the cutting end face was completed, feed 0.5mm to the Z axis, and then reverse turning was performed. The tool only needs to pass twice to complete the processing. Machining the excircle of A-B-C-D surface, with a 0.6mm depth of cut, and the tool needs two complete passes, and the third time the forward pass is completed. When the first pass of machining the end face was completed, the tool was feed 0.6 mm to the X-axis and then reverse turning was performed. Then stopped the machine to clamp the A-B-C-D face of the workpiece. The end faces of face C-D-E-F face were first machined with the same procedure as the end face of faces A-B-C-D, and then an excircle with a diameter of 48 mm and a depth of cut of 0.5 mm was machined. Hence, the tool can be completed in one complete pass machining, followed by machining an excircle with a diameter of 44mm and a depth of cut of 0.5mm. Finally, the excircle with a diameter of 40mm was processed, and the processing can be completed in two passes.

3.2.2 The processing methods and technological parameters of the second group

In the second set of experiments, the surface layer of the work blank was first cut off by 2mm to better compare the chip difference and surface quality. An excircle with a length of 30mm was processed by MDT and UDT, and the processing was grouped according to the depth of cut. The forward and reverse turning of MDT and UDT turning were performed on three separate workpieces. After one set of processing was completed, the machine was stopped for chip collection. Chip cleaning before the start of the next set of processing. The main comparison was the morphological characteristics of the chips between UDT and MDT at the same depth of cut. Measured the roughness of three workpieces to compare surface quality. The cutting parameters and processing schematic are shown in Fig. 7.
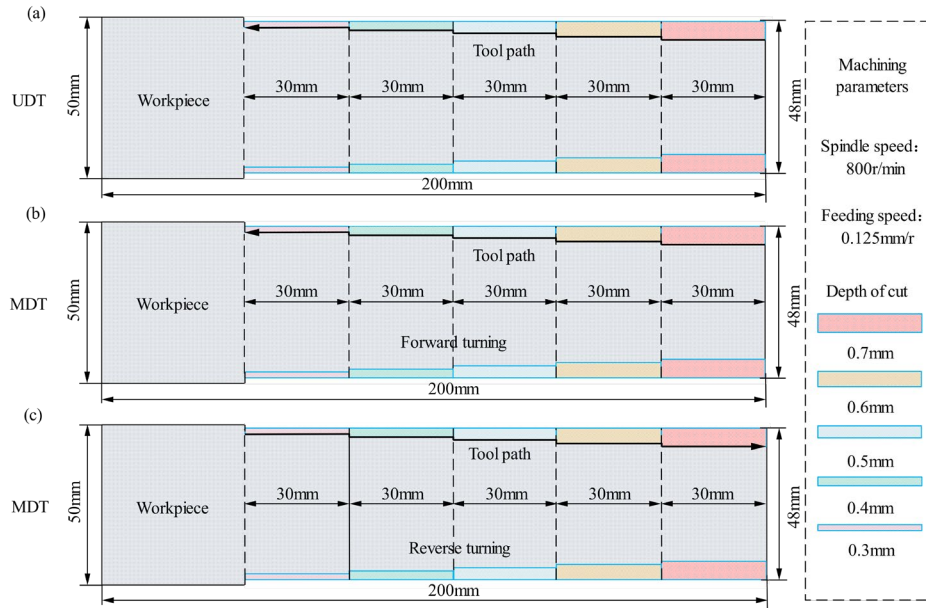
Fig. 7 Cutting parameters and processing schematic for the second group of experiments. (a) Machining schematic for the UDT; (b) Machining schematic for the forward turning of MDT; (c) Machining schematic for the reverse turning of MDT.

4 Results and discussion

The experimental results are mainly composed of four parts, processing time, energy consumption, chip morphology and workpiece roughness. The energy consumption statistics were analyzed to compare the energy efficiency of UDT and MDT, and the processing efficiency of UDT and MDT was compared through the statistics of processing time. The chip control performance of UDT and MDT was analyzed by the comparison of the chip morphology collected and the chip removal status in the processing process. The processing effect was analyzed by comparing the surface quality of processed products.

Tab.3 The energy consumption and processing time of MDT and UDT

Workpiece	Features	Energy consumption (kW·h)						Processing time (s)					
		Process		Step		Total		Process		Step		Total	
		UDT	MDT	UDT	MDT	UDT	MDT	UDT	MDT	UDT	MDT	UDT	MDT
1	A-B-C-D surface: end face Φ50	0.175	0.148	0.765	0.673			123	109	520	481		
	A-B-C-D surface: excircle Φ44	0.591	0.525					397	372				
	C-D-E-F surface: end face Φ50	0.145	0.129			1.837	1.638	123	110			1328	1243
	C-D-E-F surface: excircle Φ48	0.369	0.334	1.071	0.965			265	254	808	762		
	C-D-E-F surface: excircle Φ44	0.368	0.329					273	260				
	C-D-E-F surface: excircle Φ40	0.190	0.173					147	138				
2	G-H-I-J surface: end face Φ50	0.149	0.130	0.376	0.336			122	110	295	268		
	G-H-I-J surface: excircle Φ48	0.227	0.206					173	158				
	I-J-K-L surface: end face Φ50	0.140	0.117			2.787	2.585	122	110			2201	2015
	I-J-K-L surface: excircle Φ40	1.450	1.4217	2.411	2.249			1113	1073	1906	1747		
	I-J-K-L surface: bevel and excircle Φ30	0.821	0.710					671	564				
3	M-N-O-P surface: end face Φ25	0.028	0.024					41	35				
	M-N-O-P surface: excircle Φ22	0.210	0.190	0.371	0.336			293	277	527	488		
	M-N-O-P surface: excircle Φ20	0.091	0.082					129	117				
	M-N-O-P surface: Excircle Φ18	0.042	0.040			0.620	0.561	64	59			889	820
	O-P-Q-L surface: end face Φ25	0.028	0.024					41	35				
	O-P-Q-L surface: Excircle Φ20	0.176	0.162	0.249	0.225			255	237	362	332		
	O-P-Q-L surface: excircle Φ18	0.045	0.039					66	60				

4.1Comparative analysis of energy consumption and processing efficiency

The energy consumption and processing time of MDT and UDT are shown in Table 3. The comparison of energy consumption of each section between UDT and MDT is shown in Fig. 8. According to the comparison, the energy consumption of UDT is higher than that of MDT for processing each workpiece. In the workpiece 1, the total energy consumption of UDT is 1.837kW·h while MTD is 1.638kW·h, which compared to the 0.199kW·h reduction. In the workpiece 2, the total energy consumption of UDT is 2.787kW·h while MTD is 2.585kW·h, which compared to the 0.202kW·h reduction. In the workpiece 3, the total energy consumption of UDT is 0.62kW·h while MTD is 0.561kW·h, which compared to the 0.059kW·h reduction. The energy improvement rate of each section is shown in Fig. 10. In the workpiece 1, the energy consumption improvement rate is between 10% in each processing step. The maximum increase in energy efficiency appears when processing the end face of A-B-C-D face. The minimum increase in energy efficiency appears when processing the final excircle of C-D-E-F face. The total energy consumption improvement rate of MDT is 10.85% compared with UDT. In the workpiece 2 and 3, the total energy consumption improvement rate is 7.25% and 9.51%, respectively. The improvement in energy consumption is most significant when machining workpiece 1.
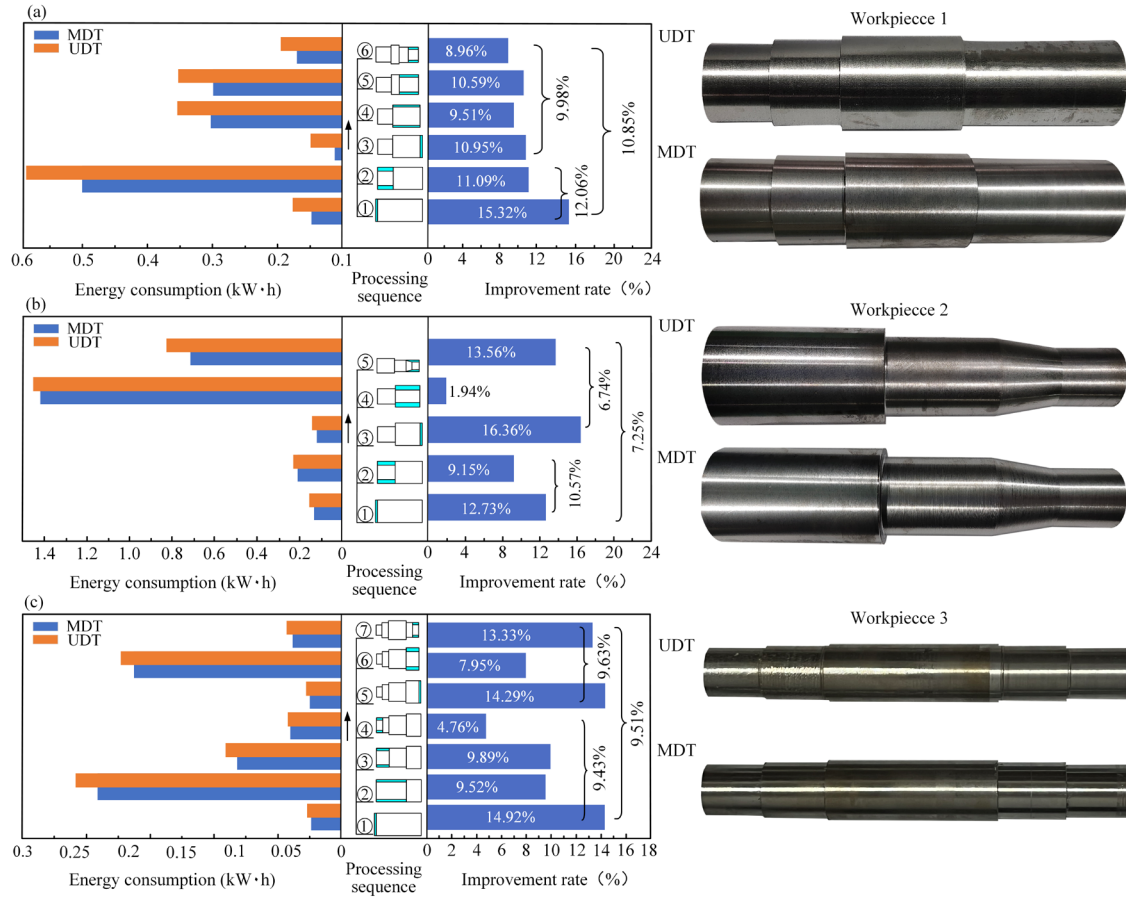
Fig. 8 The comparison of energy consumption between UDT and MDT. (a) Energy consumption and finished product of workpiece 1; (b) Energy consumption and finished product of workpiece 2; (c) Energy consumption and finished product of workpiece 3.

The comparison of processing time between UDT and MDT is shown in Fig. 9. According to the comparison, the processing time of UDT is higher than that of MDT for processing each workpiece. In the workpiece 1, the total processing time of UDT is 1328s while MTD is 1243s, which compared to the 85s reduction. In the workpiece 2, the total processing time of UDT is 2201s while MTD is 2015s, which compared to the 186s reduction. In the workpiece 3, the total processing time of UDT is 889s while MTD is 820s, which compared to the 69s reduction. The processing time improvement rate of each section is shown in Fig. 10. In the workpiece 1, the reduction of processing time is most significant when machining both end faces. When the first excircle of C-D-E-F surface is machined, the reduction of processing time is minimized. The total processing time improvement rate of MDT is 6.4% compared with UDT. In the workpiece 2 and 3, the total processing time improvement rate is 8.45% and 7.76%, respectively. The improvement rate in energy consumption is most significant when machining workpiece 2.
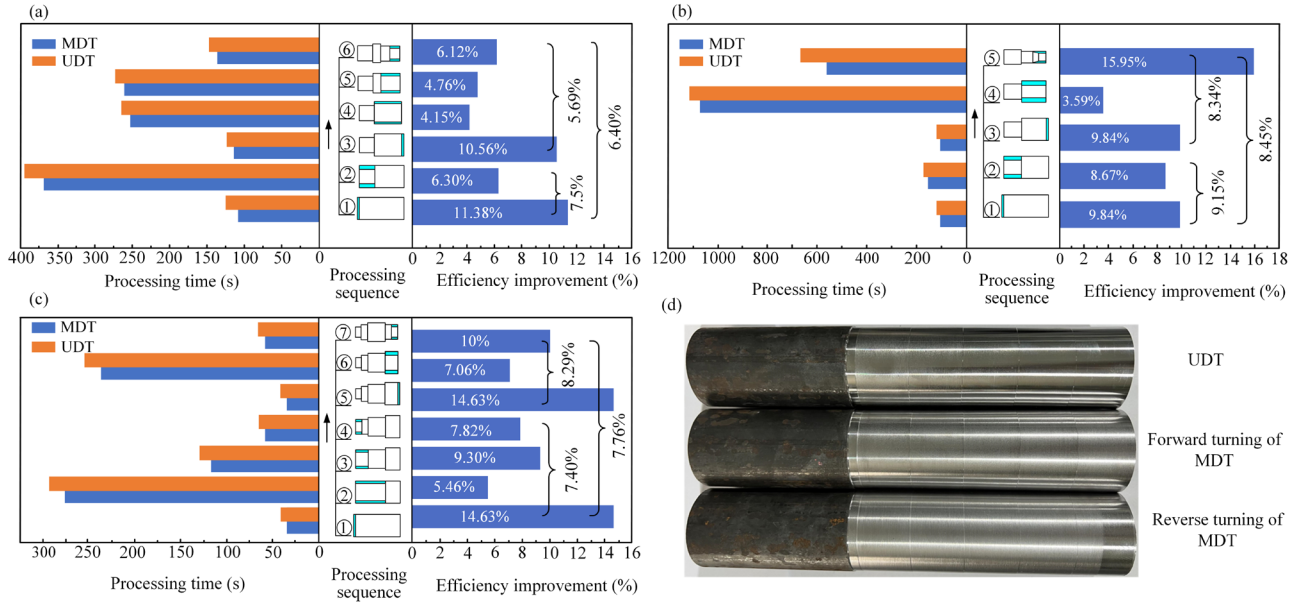
18

Fig. 9 The comparison of processing time between UDT and MDT. (a) Processing time of workpiece 1; (b) processing time of workpiece 2; (c) Pprocessing time of workpiece 3; (d) Workpiece surface for the second set of experiments.
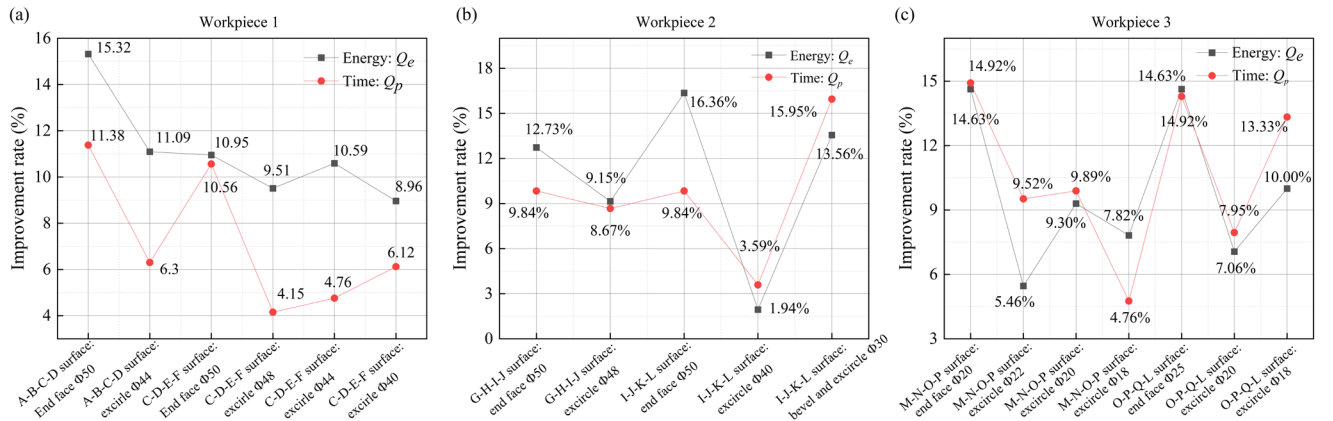

Fig. 10 The improvement rate of energy consumption and processing time for MDT. (a) Improvement rate of workpiece 1; (b) Improvement rate of workpiece 2; (c) Improvement rate of workpiece 3.

4.1.1 Differences in production efficiency and energy consumption

The power curves of machine tool when adopted UDT and MDT to machine are shown in Fig. 11. Only the power of the machine tool from the beginning to the end of cutting is retained, and some abnormal data are deleted. The material removal time of MDT and UDT is equal at the same feeding speed. Therefore, the difference of processing time between MDT and UDT appears in the tool retracting of the Z-axis and X-axis. UDT adopts one-way turning, the tool is retracted on the X axis and Z axis when the material removal is completed each time. After each processing is completed, it is accompanied by the idle running of the machine tool until the next new cutting. However, MDT can remove material in the

reverse direction, thus reducing the tool retraction time of X axis and Z axis. The power curve of the machine tool is closely connected when cutting the different steps of the workpiece. The energy saving of MDT mainly includes two aspects. Firstly, by comparing the power curves of MDT and UDT, it can be found that the average power of UDT is higher than that of MDT. This is related to the difference in the tool angle and the difference in the contact surface of the tool squeezing the workpiece during forward and reverse turning. Secondly, compared with MDT, UDT takes more time for idle tool retrenching and feeding on X-axis and Z-axis which consumes additional electrical energy.
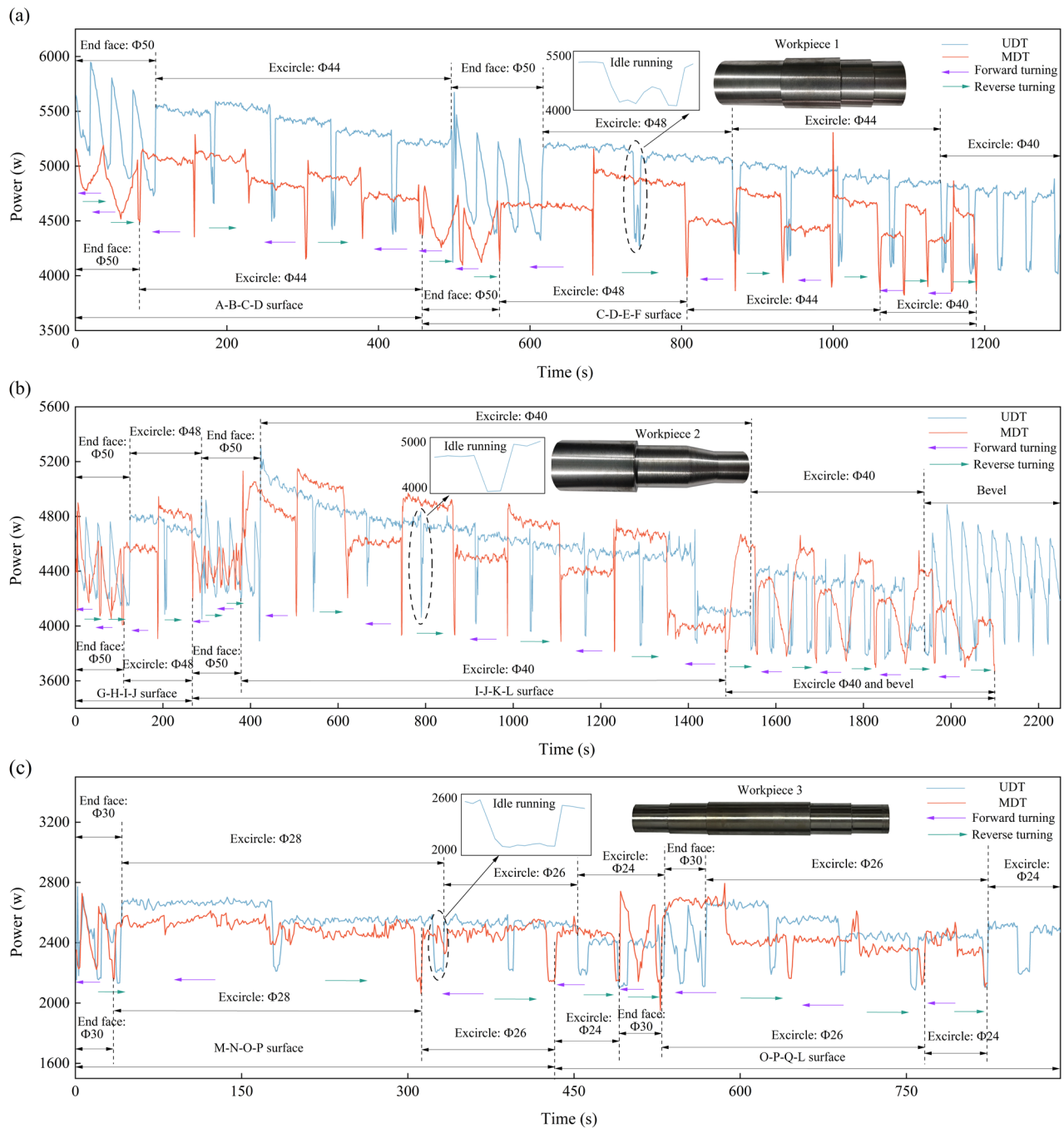

Fig. 11 The power graph of machine tool when adopted UDT and MDT to machine different workpieces. (a) Power

graph of workpiece 1; (b) Power graph of workpiece 2; (c) Power graph of workpiece 3.

The obtained energy consumption of the experiment is on one machine and there is uncertainty about the difference in energy consumption of different machines. In addition, the energy consumption of the machine is affected by the material and features of the workpiece and the use of cutting fluids, etc [6]. Machining time is influenced by workpiece features and cutting parameters. The energy saving and production efficiency of MDT requires further investigation and still has potential for development.

4.2Comparative analysis of chips and surface quality

In the first set of experiments, MDT cuts off the accumulated chips in the forward turning when reverse turning, which avoids further deterioration of the chips. In addition, the chip flow direction of MDT is stable during the reverse turning process, and there is no chip flying (Fig. 12(d)). In the UDT turning process, there is a case that the chips wrap around the workpiece and the tool. The accumulation of the chips for a long time causes them to wrap into a ball (Fig. 12(c)). In the second set of experiments, a comparative analysis of the chip morphologies is produced in the same cutting parameters. The quantization parameters of chips are shown in Fig. 12(b). For UDT, chaos chips are generated at depths of cut between 0.3mm to 0.5mm. And it was difficult to break chips. When the depths of cut reached 0.6mm and 0.7mm, the helical chip was produced. The chips become regular. Nevertheless, helical chips were presented in MDT forward cutting at depths of cut between 0.3mm and 0.7mm. The reverse turning of MDT produced helical chips (when depths of cut is 0.3 to 0.5). When depths of cut reached 0.6mm, two types of chips, helical and C, were produced. When depths of cut were 0.7mm, clockwork chips were produced. Furthermore, the chips width produced by reverse turning is wider than forward turning. The chip screw diameter of reverse turning is smaller than that of forward turning. Chip curling is more severe when reverse turning. The above shows that the reverse turning chip morphology is more stable and beneficial to machining.
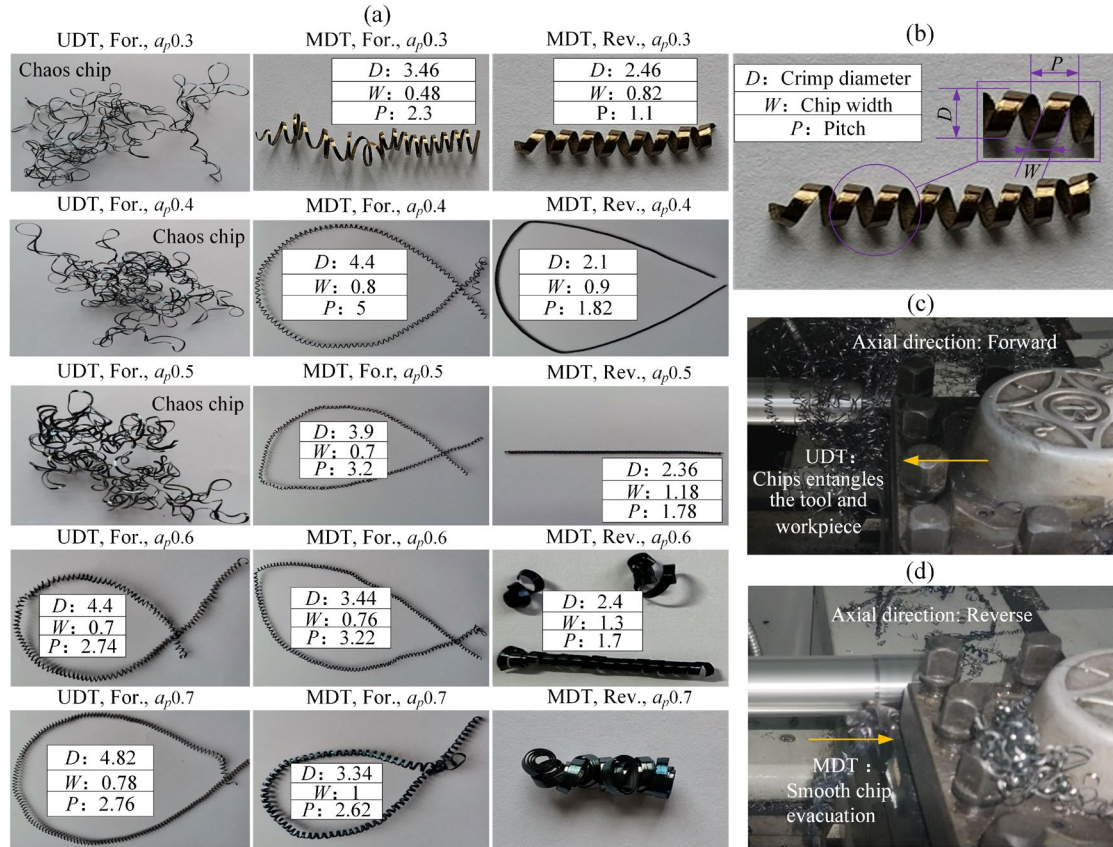
Fig. 12 The Comparison of chip removal and chip morphologies (For. stands for forward, Rev. stands for reverse.). (a) Comparison of chip morphologies; (b) The schematic diagram of chip parameters; (c) The chip removal during the conventional turning of the excircle circle; (d) The chip removal during the MDT turning of the excircle.

The roughness data include the surface quality of the three workpieces in the first set of experiments and the workpieces machined with different depth of cut in the second set of experiments. To improve the measurement accuracy, each surface of the workpiece is measured at six different positions in the radial direction, and the average value is taken. The roughness value of the three workpieces is shown in Fig. 13. The finished products of the three workpieces are shown in Fig. 8. The workpiece is not finished, and the roughness is relatively large. Nevertheless, the surface quality of the finished product processed by MDT is better than that of the UDT. The surface of the workpiece processed by MDT is smoother, and there are fewer particle stripes. The surface of the workpiece processed by UDT has a small number of burrs, which is relatively rough. The roughness value of third workpiece is the highest. Due to the thinness of the third workpiece, the machining process vibration causes a rise in roughness.
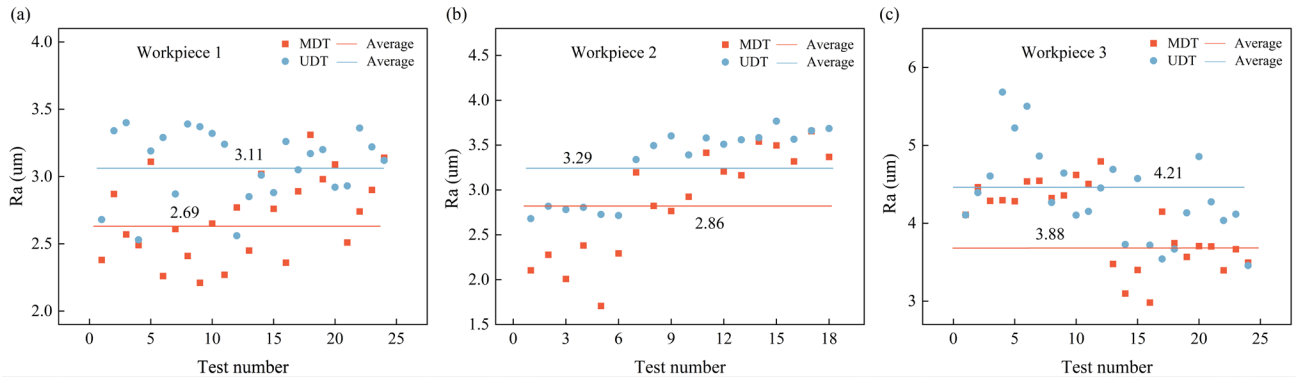
Fig. 13 The roughness value of workpiece excircle surface. (a) Roughness value of workpiece 1; (b) Roughness value of workpiece 2; (c) Roughness value of workpiece 3.

The roughness values of workpieces machined with different depth of cut in the second set of experiments is shown in Table. 4. The roughness values of UDT are higher than that of MDT for both forward turning and reverse turning. The roughness values of MDT for forward turning are lower than that of reverse turning. Therefore, the forward turning of MDT is more favorable to obtain high precision surface. In addition, the experimental procedure appeared the accident that due to the force of reverse turning and insufficient clamping force, the clamping of the workpiece is loose, and the processing fails. The clamping force needs to be increased appropriately when using MDT machining.

Tab.4 The roughness values of the second set of experiments

| Approach | | Spindle speed (r/min) | Feeding speed (mm/rev) | Depth of cut (mm) | Roughness Ra (μm) | | | | | | Average |
					Position 1	Position 2	Position 3	Position 4	Position 5	Position 6	
UDT		800	0.125	0.3	1.987	2.192	2.53	2.472	2.422	2.271	2.312
				0.4	2.938	2.167	1.443	2.396	1.966	1.972	2.147
				0.5	1.279	1.627	1.846	1.451	1.809	1.737	1.625
				0.6	1.222	2.104	1.958	1.627	2.338	1.710	1.827
				0.7	0.903	2.343	2.005	2.121	1.981	1.879	1.872
MDT	Forward turning	800	0.125	0.3	1.521	1.615	1.040	0.792	1.683	0.897	1.258
				0.4	1.389	1.227	1.541	1.287	1.221	1.252	1.320
				0.5	1.269	1.283	1.411	1.341	1.443	1.218	1.328
				0.6	1.179	1.254	1.272	1.402	1.381	1.238	1.288
				0.7	1.385	1.398	1.390	1.387	1.471	1.152	1.364
	Reverse turning			0.3	2.222	2.108	1.968	1.906	1.741	1.541	1.914
				0.4	1.287	1.578	1.553	1.389	1.515	1.523	1.474
				0.5	1.443	1.448	1.545	1.583	1.461	1.484	1.494
				0.6	1.394	1.350	1.341	1.440	1.422	1.349	1.383
				0.7	1.446	1.429	1.369	1.389	1.388	1.461	1.414

4.2.1Differences in chips and surface quality

The forward turning process of MDT and UDT with a large tool cutting edge angle, and the chips produced are mainly slender and curled. In the reverse turning process of MDT, the tool cutting edge angle is small, so the chips generated are wider and thinner, at the same time, the chip removal during the reverse turning process is stable and the chip breaking is more uniform. The material of the UDT tool is the same as that of the MDT tool, and the same depth of cut and spindle speed are used in the turning process. UDT adopted a negative edge angle, causing chips to flow to the machined surface, which leads to scratches on the surface of the workpiece. Meanwhile, MDT adopted a small tool cutting edge angle during the reverse turning process to produce chips that have better heat dissipation capabilities. It can suppress the formation of built-up edge during processing. The radial force of reverse turning increases, causing the workpiece to vibrate stronger and leading to higher roughness.

The chip formation and surface quality in relation to workpiece material, which also influenced by the cutting parameters and cutting fluid, etc. In actual conventional turning operation, the machine is stopped due to chip tangling, which leads to more time and energy consumption [40]. The effect of MDT on the surface quality and chip formation requires further comprehensive comparative study.

In actual machining, MDT shows its superiority compared to UDT, but there are also some limitations. First of all, in the reverse turning process of MDT, due to the change of the direction of the cutting axial force on the workpiece, it may cause looseness between the triangular chuck and the workpiece which leads to the failure of processing. In severe cases, the workpiece may be thrown off and cause damage to the machine tool and the operator. Therefore, it is necessary to increase the clamping force on the workpiece, especially when processing some workpieces with poor rigidity. The reverse turning process causes machine chatter to be more pronounced than forward machining due to the increased radial forces.

5 Conclusions

To establish an energy efficient turning approach (MDT) to promote sustainable development in manufacturing. The energy consumption and processing efficiency models of MDT and UDT were analyzed. Through a case study, MDT has shown superiority over UDT in terms of energy savings and improved processing efficiency.

In the case study, MDT through reducing idle energy consumption and machine power can maximum

improve the energy efficiency by 10.85%. The large number of lathes in the industrial field is accompanied by huge energy consumption. Thus, through the application of the MDT approach on the lathe, it will be expected to save huge energy consumption. However, in the actual processing of multiple materials and features, the actual energy efficiency of MDT still needs to be investigated.

For the same part processing, the production efficiency of MDT maximum increased by 8.86%, which will fulfill the requirements of enterprises to increase machine tool production and increase corporate benefits. For the machining of complex parts in actual production, the processing efficiency of MDT is expected to be further expanded, but it is yet to be investigated.

Under the same cutting parameters, the surface quality of the finished product obtained by MDT is better than that of the parts obtained by UDT. MDT forward turning provides better surface quality compared to reverse turning. Furthermore, the MDT approach shows better chip control characteristics during the processing, especially in the reverse turning process. Therefore, MDT is a more stable and effective processing approach to balance surface quality and efficiency.

In summary, this study concerns a novel turning approach of MDT to improve energy efficiency and increase processing efficiency. It was verified through multiple sets of experiments, which provides a certain theoretical guiding significance for its use in actual production. As two contradictory elements [41-42], the energy consumption and surface roughness of MDT need further comprehensive study.

Acknowledgments

References

[1] Tian G, Yuan G, Aleksandrov A, et al. Recycling of spent Lithium-ion Batteries: A comprehensive review for identification of main challenges and future research trends. Sustainable energy technologies and assessments. 2022; 53: 102447.

[2] Cao Y, Li XM, Yan HB, et al. China's Efforts to Peak Carbon Emissions: Targets and Practice. Chinese journal of urban and environmental studies. 2021; 9(1): 2150004.

[3] Zou CN, Xiong B, Xue HQ, Zheng DW, et al. The role of role new energy in carbon neutral. Petroleum

exploration and development. 2021; 48(2): 480-491.

[4] Hu L, Tang R, Cai W, et al. Optimization of cutting parameters for improving energy efficiency in machining process. Robotics and Computer-Integrated Manufacturing. 2019; 59: 406-416.

[5] He C. Zong w j, Zhang J J. Influencing factors and theoretical modeling methods of surface roughness in turning process: State-of-the-art. International Journal of Machine Tools and Manufacture. 2018; 129: 15-26.

[6] Zhao GY, Liu ZY, He Y, et al. Energy consumption in machining: Classification, prediction, and reduction strategy. Energy. 2017; 133: 142-157.

[7] Cai W, Liu F, Xie j, et al. A tool for assessing the energy demand and efficiency of machining systems: energy benchmarking. Energy. 2017; 138: 332-347.

[8] Tian C, Zhou G, Lu Q, et al. An integrated decision-making approach on cutting tools and cutting parameters for machining features considering carbon emissions. International Journal of Computer Integrated Manufacturing. 2019; 32(7): 629-641.

[9] Luan X, Zhang S, Chen J, et al. Energy modelling and energy saving strategy analysis of a machine tool during non-cutting status. International Journal of Production Research. 2019; 57(14): 4451-4467.

[10] Luo H, Wang Y, Zhang P. Effect of cutting parameters on machinability of 7075-T651 aluminum alloy in different processing methods. The International Journal of Advanced Manufacturing Technology. 2020; 110(7): 2035-2047.

[11] Petrů, J, Zlámal T, Čep R, et al. The effect of feed rate on durability and wear of exchangeable cutting inserts during cutting Ni-625. TEHNICKI VJESNIK-TECHNICAL GAZETTE. Supplement. 2017; 24: 1-6.

[12] Devin L N, Stakhniv N E, Antoniuk a s, et al. The influence of cutting speed on cutting temperatures and forces in fine turning of VT1-0 titanium alloy by a PCD tool. Journal of Superhard Materials. 2019; 41(2): 119-125.

[13] Basmaci G. Optimization of Machining Parameters for the Turning Process of AISI 316 L Stainless Steel and Taguchi Design. Acta Physica Polonica A. 2018; 134(1): 260-264.

[14] Arfaoui S, Zemzemi F, Dakhli M, et al. Optimization of Hard Turning Process Parameters using the Response Surface Methodology and Finite Element Simulations. International Journal of Advanced Manufacturing Technology. 2019; 103(1-4): 1279-1290.

[15] Cai W, Li Y, Li L, et al. Energy saving and high efficiency production oriented forward-and-reverse multidirectional turning: Energy modeling and application. Energy. 2022,252:123981.

[16] Lv J, Peng T, Tang R. Energy modeling and a method for reducing energy loss due to cutting load during machining operations. Proceedings of the Institution of Mechanical Engineers. Part B, Journal of engineering manufacture. 2019; 233: 699-710.

[17] Moradnazhad M, Unver HO. Energy consumption characteristics of turn-mill machining. International journal of advanced manufacturing technology. 2016; 91:1991-2016.

[18] Lv J, Tang R, Tang W, et al. An investigation into methods for predicting material removal energy

consumption in turning. Journal of cleaner production. 2018; 193: 128-139.

[19] Shin S, Woo J, Rachuri S, et al. Standard Data-Based Predictive Modeling for Power Consumption in Turning Machining. Sustainability. 2018; 10: 598.

[20] Zhao G, Hou C, Qiao J, et al. Energy consumption characteristics evaluation method in turning. Advances in mechanical engineering. 2016; 8.

[21] Su Y, Li CB, Zhao GY, er at. Prediction models for specific energy consumption of machine tools and surface roughness based on cutting parameters and tool wear. 2021; 235(6-7): 1225-1234.

[22] Wang Q, Zhang D, Chen B, et al. Energy Consumption Model for Drilling Processes Based on Cutting Force. Applied sciences. 2019; 9: 4801.

[23] Lv J, Tang R, Tang W, et al. An investigation into reducing the spindle acceleration energy consumption of machine tools. Journal of cleaner production. 2017; 143: 794-803.

[24] Zhong Q, Tang R, Lv J, et al. Evaluation on models of calculating energy consumption in metal cutting processes: a case of external turning process. International journal of advanced manufacturing technology. 2015; 82: 2087-2099.

[25] Pawanr S, Garg GK, Routroy S. Development of an Empirical Model for Variable Power Consumption Machining Processes: A Case of End Facing. Arabian journal for science and engineering. 2021.

[26] Warsi SS, Jaffery SHI, Ahmad R, et al. Development of energy consumption map for orthogonal machining of Al 6061-T6 alloy. Proceedings of the Institution of Mechanical Engineers. Part B, Journal of engineering manufacture. 2018; 232: 2510-2522.

[27] Cui X, Zhao B, Jiao F, et al. Formation characteristics of the chip and damage equivalent stress of the cutting tool in high-speed intermittent cutting. The International Journal of Advanced Manufacturing Technology. 2017; 91(5): 2113-2123.

[28] Shi Chenchun, Aibing Yu, Jianzhao Wu, et al. Study on Position of Laser Cladded Chip Breaking Dot on Rake Face of HSS Turning Tool. International Journal of Machine Tools & Manufacture. 2017; 122: 132-148.

[29] Chiappini Elio, Stefano Tirelli, Paolo Albertelli, et al. On the Mechanics of Chip Formation in Ti–6Al–4V Turning with Spindle Speed Variation. International Journal of Machine Tools & Manufacture. 2014; 77: 16-26.

[30] Sutter G, G List. Very high speed cutting of Ti–6Al–4V Titanium Alloy – Change in morphology and mechanism of chip formation. International Journal of Machine Tools & Manufacture. 2013; 66: 37-43.

[31] Molnar Tamas G, Berezvai Szabolcs, Kiss Adam K, et al. Experimental Investigation of Dynamic Chip Formation in Orthogonal Cutting. International Journal of Machine Tools & Manufacture. 2019; 145: 103429.

[32] Mabrouki Tarek, Courbon Cédric, Zhang Yancheng, et al. Some Insights on the Modelling of Chip Formation and its Morphology during Metal Cutting Operations. Comptes Rendus Mecanique. 2016; 344(4-5): 335-354.

[33] Moreira L C, Li W D, Lu X, et al. Energy-Efficient machining process analysis and optimization based on BS EN24T alloy steel as case studies. Robotics and Computer-Integrated Manufacturing. 2019; 58: 1-12.

[34] Hu L, Tang R, Cai W, et al. Optimization of cutting parameters for improving energy efficiency in machining process. Robotics and Computer-Integrated Manufacturing. 2019; 59: 406-416.

[35] Chen X, Li C, Tang Y, et al. Integrated optimization of cutting tool and cutting parameters in face milling for minimizing energy footprint and production time. Energy. 2019; 175: 1021-1037.

[36] Zhong Q, Tang R, Peng T. Decision rules for energy consumption minimization during material removal process in turning. Journal of cleaner production. 2017; 140: 1819-1827.

[37] Hu L, Liu Y, Lohse N, et al. Sequencing the features to minimise the non-cutting energy consumption in machining considering the change of spindle rotation speed. Energy. 2017; 139: 935-946.

[38] Migranov M S, Migranov A M, Minigaleev S M, et al. Tribological properties of multilayer coatings for cutting tool. Journal of Friction and Wear. 2018; 39(3): 245-250.

[39] Cai W, Wang L, Li L, et al. A review on methods of energy performance improvement towards sustainable manufacturing from perspectives of energy monitoring, evaluation, optimization and benchmarking. Renewable & sustainable energy reviews. 159.

[40] Buchkremer S, Klocke F, Veselovac D. 3D FEM simulation of chip breakage in metal cutting. International journal of advanced manufacturing technology. 2015; 82: 645-661.

[41] Kahya M, Ozbayoglu M, Unver HO. Precision and energy-efficient ball-end milling of Ti6Al4V turbine blades using particle swarm optimization. International journal of computer integrated manufacturing. 2021; 34: 110-133.

[42] Serin G, Ozbayoglu M, Unver HO. Integrated energy-efficient machining of rotary impellers and multi-objective optimization. Materials and manufacturing processes. 2020; 35: 478-490.